Available online at www.sciencedirect.com
SCIENCE DIRECT
Journal of Catalysis 234 (2005) 414–420
JOURNAL OF CATALYSIS
www.elsevier.com/locate/jcat

^{31}P MAS NMR and Raman study of a Co(Zn)MoP/γ-Al_2O_3 HDS catalyst precursor containing triethylene glycol

Daniele Nicosia, Roel Prins *

Institute of Chemical and Bioengineering, Federal Institute of Technology (ETH), 8093 Zurich, Switzerland

Received 12 April 2005; revised 4 July 2005; accepted 7 July 2005

Available online 11 August 2005

Abstract

The effect of triethylene glycol on phosphate-doped Co(Zn)Mo catalysts supported on γ-Al_2O_3 was studied by means of ^{31}P magic angle spinning nuclear magnetic resonance (MAS NMR) and Raman spectroscopy. ^{31}P MAS NMR experiments, carried out on ZnMo/γ-Al_2O_3 doped with phosphate and triethylene glycol, suggested that the $P_2Mo_5O_{23}^{6-}$ species that formed in the impregnation solution decomposed to monophosphate and an Anderson-type aluminum molybdate species on contact with the support. The presence of triethylene glycol favored the formation of polyphosphate and $PMo_{12}O_{40}^{3-}$ heteropolymolybdate species, but no $P_2Mo_5O_{23}^{6-}$ was detected. The use of paramagnetic cobalt instead of zinc cations had a paramagnetic effect on the ^{31}P-NMR signal of the $PMo_{12}O_{40}^{3-}$, indicating that the $PMo_{12}O_{40}^{3-}$ species are bound to the promoter atoms. The close proximity of the promoter and Mo allows a better decoration of MoS_2 and improves the catalytic activity.
© 2005 Elsevier Inc. All rights reserved.

Keywords: CoMo hydrotreating catalyst; Phosphomolybdates; ^{31}P MAS NMR; Paramagnetic effect of Co(II); Triethylene glycol; Raman

1. Introduction

Conventional hydrotreating catalysts are composed of cobalt and molybdenum supported on an inert support, such as γ-Al_2O_3, and can be prepared by depositing oxidic cobalt and molybdenum precursors on the support. The oxidic precursors are then presulfided at 400 °C using a mixture of H_2 and H_2S. To improve the catalytic activity of the catalysts, chelating ligands or phosphate, for example, can be added during the preparation of the catalyst [1–3]. When phosphate is added to the impregnation solution, it reacts with the molybdenum precursor and, depending on the reaction conditions, gives rise to a variety of phosphomolybdate anions, including Keggin ($PMo_{12}O_{40}^{3-}$, $PMo_{12}O_{40}^{7-}$), Dawson ($P_2Mo_{18}O_{62}^{6-}$), and diphospho-pentamolybdate ($P_2Mo_5O_{23}^{6-}$) anions [3,4]. Depending on the structure of the phosphomolybdate anions, the cobalt or nickel promoter cations stay in solution as a solvated aquo-complex or become complexed by the phosphomolybdate anions. Griboval et al. reported that using $Co_xH_{(6-2x)}P_2Mo_5O_{23}$ as a catalyst precursor favors a higher Co/Mo atomic ratio in the final sulfided catalyst and improves the promotion of the active phase because of the better decoration of the cobalt on the MoS_2 edge [5,6]. The adsorption of phosphomolybdates on a support has been described in detail. Cheng and Luthra reported that $PMo_{12}O_{40}^{3-}$ ions adsorb intact [7], whereas van Veen et al. and Kraus and Prins reported that the $P_2Mo_5O_{23}^{6-}$ ion decomposes to $AlPO_4$ and molybdate on adsorption on γ-Al_2O_3 [8,9].

A recently published patent claims that the addition of phosphate and glycols during catalyst preparation leads to highly active Co–Mo hydrodesulfurization catalysts [10]. We characterized the oxidic CoMo catalyst precursor containing phosphate and triethylene glycol (TEG) and prepared according to this patent recipe [11]. We found that TEG strongly interacts with the γ-Al_2O_3 support and thus prevents the decomposition of a Co-phosphomolybdate com-

* Corresponding author. Fax: +41-1-6321162.
E-mail address: roel.prins@chem.ethz.ch (R. Prins).

0021-9517/$ – see front matter © 2005 Elsevier Inc. All rights reserved.
doi:10.1016/j.jcat.2005.07.011

plex during drying. As explained by Griboval et al., promotion of the active phase is thus improved because of the better cobalt decoration on the MoS_2 edge.

Here we describe the effect of TEG on the structure of the oxidic catalysts doped with phosphate as determined by ^{31}P nuclear magnetic resonance (NMR) and Raman experiments on Zn(Co)Mo catalysts supported on γ-Al_2O_3. When a paramagnetic atom or ion is in close proximity to an atom, broadening and shifting of the NMR signals of this atom are typically observed. Because cobalt and nickel ions are paramagnetic, NMR has rarely been used for hydrotreating catalysts. However, De Canio et al. [12] and Kraus and Prins [13] used the paramagnetic effect to estimate the proximity of cobalt (or nickel) to various elements. The use of diamagnetic Zn instead of Co cations avoids the paramagnetic effect on the NMR signal, thus allowing better interpretation of the spectra. Therefore, we compared the ^{31}P NMR of samples containing paramagnetic cobalt and diamagnetic zinc cations. Together with Raman measurements, these experiments provided insight into the role of TEG in phosphate-containing CoMo-supported catalysts.

2. Experimental

By means of wet impregnation, CoMoP and CoMoP-TEG catalysts, supported on γ-Al_2O_3, were prepared according to the European patent application 0601722 B1 [10] and our previous work [11]. ZnMoP and ZnMoP-TEG reference samples were prepared as described previously [12] for the corresponding Co-containing solutions, by dissolving 0.9 g $Zn_5(CO_3)_2(OH)_6{\cdot}7H_2O$ (1.6 mmol, Aldrich p.a.), 2.7 g MoO_3 powder (18.7 mmol, Fluka, purum, p.a.), 0.5 ml of an 85 wt% aqueous H_3PO_4 solution (7.5 mmol H_3PO_4, Aldrich, p.a.), and 2 ml of TEG (15 mmol, Aldrich, p.a.) in 10 ml of water [11]. The final solution was light green in color and had a pH of 2.5.

Before impregnation with one of the impregnating solutions, γ-Al_2O_3 (Condea Chemie) and the γ-Al_2O_3 support, impregnated with 0.8 ml of a 20% aqueous solution of TEG (pH adjusted to 2.5 by adding 35% HCl), were crushed, sieved to 90–125 μm grain size, and dried overnight in an oven at 120 °C. HCl was added to the TEG solution to obtain the same pH value as the original impregnation solution. The total water pore volume of γ-Al_2O_3 was 0.9 ml/g (the gas pore volume determined by BET was 0.45 ml/g; Table 1), and that of γ-Al_2O_3 + TEG was 0.4 ml/g. We used the same metal loading to compare samples prepared using the γ-Al_2O_3 + TEG support with the other catalysts; therefore, the γ-Al_2O_3 + TEG support had to be impregnated twice with 0.4 ml of the impregnation solution, as described previously [11]. After impregnation, the wet powder was dried overnight at 120 °C at a heating rate of 2 °C/min. All catalysts were prepared without applying calcination. Table 1 lists the investigated catalyst precursors. Elemental analysis of Co, Zn, Mo, and P, as well as nitrogen adsorption measurements of the dried but not calcined samples, were performed as described elsewhere [11].

Table 1
Hydrotreating catalysts

Catalyst	Loading (wt%)			BET s.a. (m^2/g)	P.V. (cm^3/g)
	Mo	Co(Zn)	P		
CoMoP/γ-Al_2O_3	12.85	2.88	1.75	144	0.32
CoMoP-TEG/γ-Al_2O_3	12.47	2.86	1.60	114	0.28
CoMoP/γ-Al_2O_3 + TEG	10.71	2.64	1.51	101	0.20
ZnMoP/γ-Al_2O_3	12.01	2.90	1.41	150	0.31
ZnMoP-TEG/γ-Al_2O_3	11.80	2.50	1.40	110	0.19
ZnMoP/γ-Al_2O_3 + TEG	11.00	2.4	1.35	105	0.23
γ-Al_2O_3 + TEG	–	–	–	160	0.35
γ-Al_2O_3	–	–	–	210	0.45

The nitrogen adsorption measurements were performed at liquid-nitrogen temperature with a Micromeritics TriStar 3000 device. Before measurement, the samples were degassed at 200 °C (not at 400 °C, to prevent the decomposition of the TEG) at 10 Pa overnight. For the measurements of the γ-Al_2O_3 support, the degassing was carried out at 400 °C. ^{31}P mass absorption spectroscopy (MAS) experiments were carried out on a Bruker AMX-400 FT-NMR spectrometer at a magnetic field of 9.4 Tesla using a 4-mm CP-MAS probe head, with a resonance frequency of 161.98 MHz, spinning frequency of 12 kHz, and recycle delay of 1 s. The final spectrum resulted from the accumulation of 2000 transients. The chemical shift was referenced to $NH_4H_2PO_4$ (Fluka Purum, p.a.) (0 ppm).

Raman measurements of the samples and of reference compounds were performed on a Bruker Equinox 55 spectrometer equipped with a FT-Raman-Module FRA 106/S, a Nd:YAG laser (1064 nm, 300 mW), a CaF_2 beam-splitter, and a Ge detector (D418-S) cooled by liquid nitrogen. The powder was pressed into an aluminum disk. The number of accumulated spectra of each sample was 4096. To prevent any effect induced to the specimen by the laser, we used a defocused low-power laser beam.

3. Results

3.1. ^{31}P NMR: The effect of TEG on ZnMoP/γ-Al_2O_3

^{31}P NMR spectra of the ZnMoP/γ-Al_2O_3, ZnMoP-TEG/γ-Al_2O_3, and ZnMoP/γ-Al_2O_3 + TEG samples were compared with the spectrum of a PO_4/γ-Al_2O_3 reference sample (Fig. 1). The ^{31}P NMR spectra of ZnMoP/γ-Al_2O_3 and PO_4/γ-Al_2O_3 were almost identical, showing a broad band at around −8.2 ppm, typical of isolated phosphate ions on γ-Al_2O_3 [14]. The ^{31}P NMR spectra of ZnMoP-TEG/γ-Al_2O_3 and ZnMoP/γ-Al_2O_3 + TEG showed a broad band with maximum at around −10 ppm and a sharp peak at around −5 ppm. The spectrum of ZnMoP/γ-Al_2O_3 + TEG also showed a sharp shoulder at around 0 ppm.

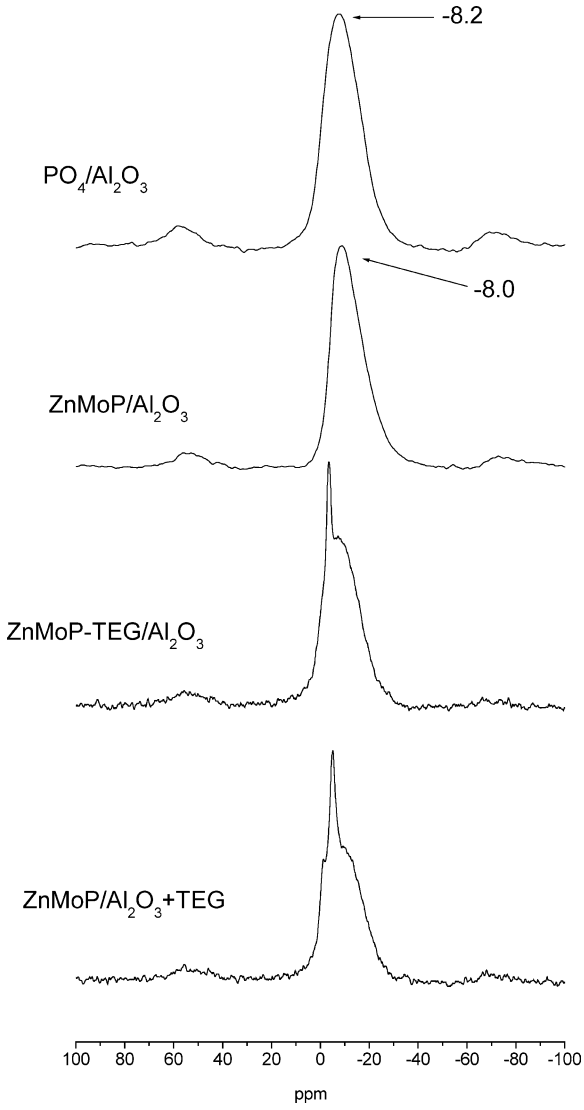

Fig. 1. ^{31}P MAS NMR spectra of PO_4/γ-Al_2O_3, ZnMoP/γ-Al_2O_3, ZnMoP-TEG/γ-Al_2O_3, and ZnMoP/γ-Al_2O_3 + TEG.

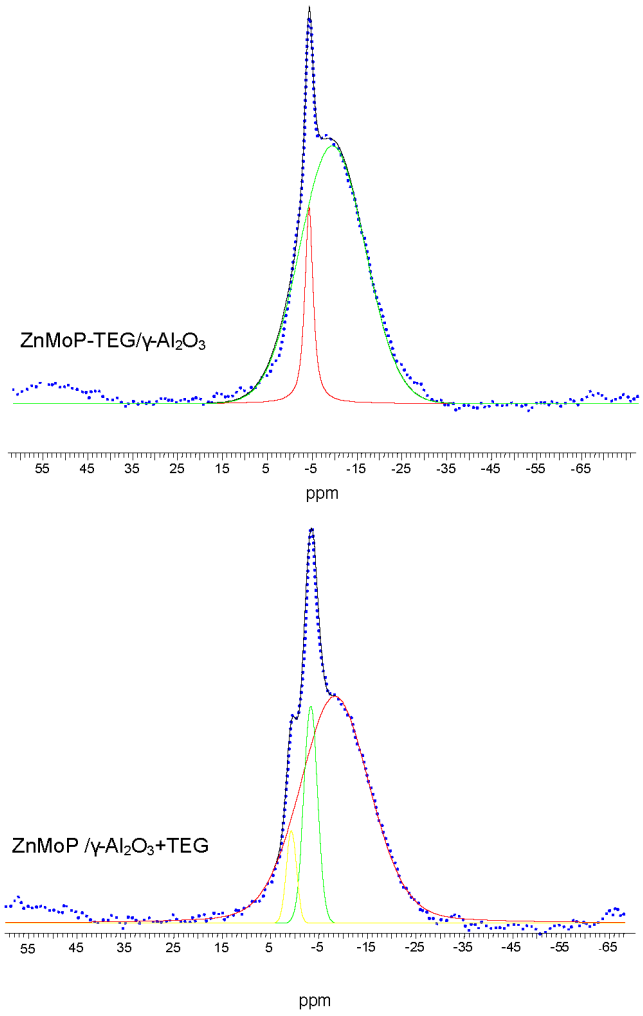

Fig. 2. ^{31}P MAS NMR spectra (···) of ZnMoP-TEG/γ-Al_2O_3 and ZnMoP/γ-Al_2O_3 + TEG and deconvolution (—).

To elucidate the nature of the phosphorus atoms, which give rise to the sharp resonance peak in the ^{31}P NMR spectra of ZnMoP-TEG/γ-Al_2O_3 and ZnMoP/γ-Al_2O_3 + TEG, we performed a deconvolution analysis of the spectra (Fig. 2; Table 2). The spectrum of the ZnMoP-TEG/γ-Al_2O_3 was deconvoluted in two contributions at −4.5 and −9.6 ppm (Table 2). The signal at −4.5 ppm may arise from $PMo_{12}O_{40}^{3-}$ [15]. The possibility that this signal may have arisen from an isolated zinc phosphate salt was ruled out, because Cheethan et al. reported that the phosphorus signals are between 0 and 10 ppm for α-$Zn_3(PO_4)_2$ and β-$Zn_3(PO_4)_2$ and between −10 and −20 ppm for α-$Zn_2P_2O_7$ [16]. The broad signal at −9.6 ppm was assigned to polyphosphate [14]. The signal of ZnMoP/γ-Al_2O_3 + TEG was deconvoluted into three signals at −1, −4.7, and −9.6 ppm (Fig. 2; Table 2). The signals at −9.6 and −4.7 ppm belong to polyphosphate and $PMo_{12}O_{40}^{3-}$, respectively, whereas the signal at −1 ppm may arise from isolated $H_2PO_4^-$. The analysis of the peak areas (Table 2) shows that >80% of the phosphorus atoms in both TEG-containing samples are present as polyphosphate, and about 15% are present as $PMo_{12}O_{40}^{3-}$.

Table 2
MAS ^{31}P NMR deconvolution results

Sample	δ (ppm)	Linewidth (kHz)	Integral rel. (%)
ZnMoP-TEG/γ-Al_2O_3	−4.5	1.0	14
	−9.6	2.6	86
ZnMoP/γ-Al_2O_3 + TEG	−1.0	0.4	3
	−4.7	0.8	15
	−9.6	2.8	82

3.2. ^{31}P NMR: The effect of TEG in CoMoP/γ-Al_2O_3

The paramagnetism of Co(II) has been used in NMR spectroscopy to check for the presence of Co^{2+} in the neighborhood of the probing nuclei [17]. When cobalt is in close proximity to the probing atom, it causes broadening and

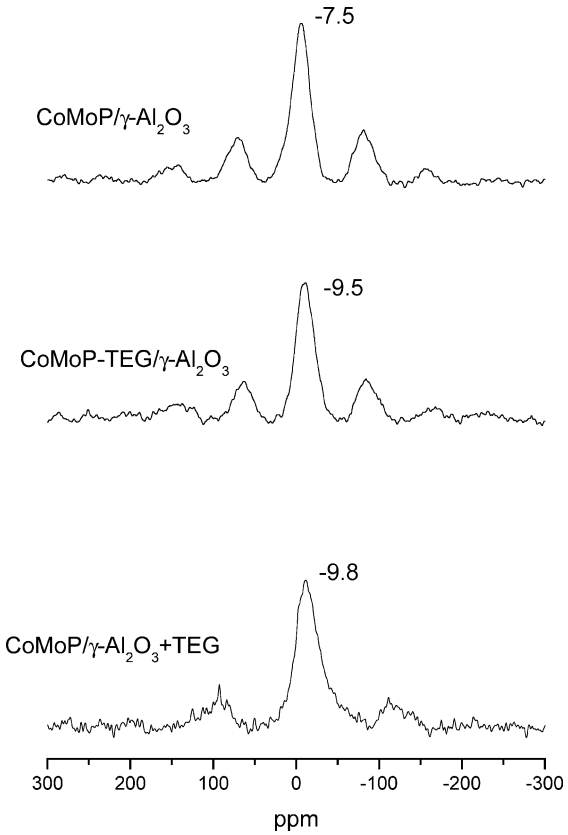

Fig. 3. ^{31}P MAS NMR spectra of CoMoP/γ-Al_2O_3, CoMoP-TEG/γ-Al_2O_3, and CoMoP/γ-Al_2O_3 + TEG.

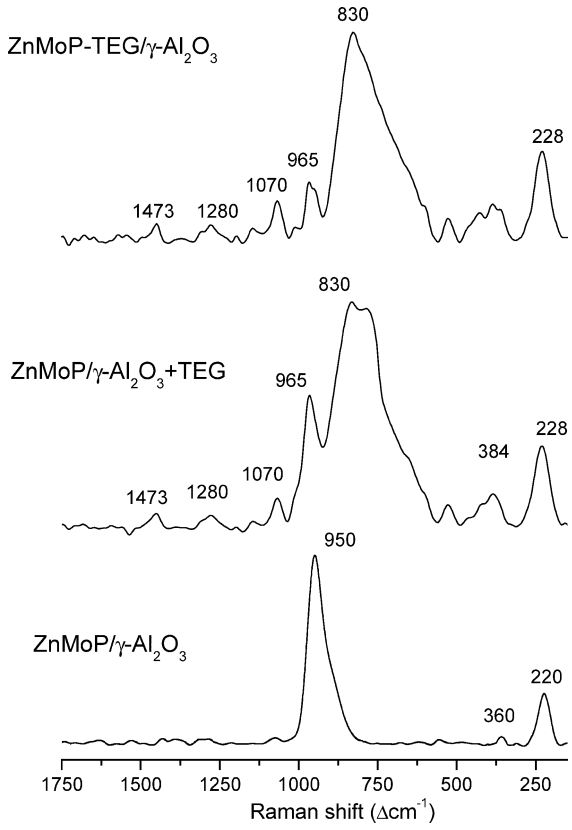

Fig. 4. Raman spectra of ZnMoP-TEG/γ-Al_2O_3, ZnMoP/γ-Al_2O_3 + TEG, and ZnMoP-TEG/γ-Al_2O_3.

shifting of the NMR signals. Because of their high magnetic moment, paramagnetic cobalt ions strongly decrease the relaxation time of phosphorus; consequently, the ^{31}P NMR peaks become broader. The peaks also shift in proportion to the electron density of Co^{2+} on the ^{31}P nucleus. Therefore, the higher the number of Co ions around a P atom, the stronger the paramagnetic effect. Comparison of the ^{31}P NMR spectrum of the PO_4/γ-Al_2O_3 sample with the ^{31}P NMR spectra of the CoMoP/γ-Al_2O_3, CoMoP-TEG/γ-Al_2O_3, and CoMoP/γ-Al_2O_3 + TEG samples shows that all of the spectra had a broad signal between 50 and −50 ppm with two side bands on either side of the central peak. However, whereas the main signal of the CoMoP/γ-Al_2O_3 showed an isotropic chemical shift of −7.5 ppm, close to that of PO_4/γ-Al_2O_3 and ZnMoP/γ-Al_2O_3, the main ^{31}P-NMR signal of the other two Co-containing samples shifted to a higher field (−9.5 ppm). There was no sharp peak between 0 and −10 ppm in the ^{31}P NMR spectra of CoMoP-TEG/γ-Al_2O_3 and CoMoP/γ-Al_2O_3 + TEG.

3.3. Laser Raman spectroscopy

Laser Raman spectroscopy (LRS) is a very sensitive technique for probing the chemical state of molybdenum. The CoMoP and ZnMoP impregnation solutions gave exactly the same LRS spectrum, which is typical of the $P_2Mo_5O_{23}^{6-}$ complex [18]; as we showed in previous work, the presence of TEG did not affect the formation of this species [11].

Fig. 4 gives the LRS spectra of ZnMoP/γ-Al_2O_3, ZnMoP/γ-Al_2O_3 + TEG, and ZnMoP-TEG/γ-Al_2O_3. The spectrum of ZnMoP/γ-Al_2O_3 has an intense band between 1000 and 850 cm^{-1}, composed of a main peak at 950 and a shoulder at about 900 cm^{-1}. Two signals are present at 360 and 220 cm^{-1}. According to the literature, these three signals can be attributed to the $Al(OH)_6Mo_6O_{18}^{3-}$ species [19]. The LRS spectra of the ZnMoP/γ-Al_2O_3 + TEG and ZnMoP-TEG/γ-Al_2O_3 samples are similar but very different from the spectrum of the TEG-free sample (Fig. 4). The peak at 1070 cm^{-1} is typical of polyphosphate [1]. The spectrum of ZnMoP-TEG/γ-Al_2O_3 showed a broad asymmetric signal with a peak at 830 cm^{-1}. This signal and the weak signals at 1473 and 1280 cm^{-1} were assigned to the presence of TEG [11], the C–O vibration of which gives rise to the signal at 830 cm^{-1}. The same TEG signals at 830, 1280, and 1473 cm^{-1} also were detected in the spectrum of ZnMoP/γ-Al_2O_3 + TEG (Fig. 4). In the region between 1000 and 950 cm^{-1} a signal corresponding to a molybdate species was detected. Unfortunately, the broadness of this signal prevents us from definitively identifying the molybdate species present in the dried samples. Moreover, the broad lines of TEG located at about 830 cm^{-1} make the interpretation even more uncertain. Even though we tried to

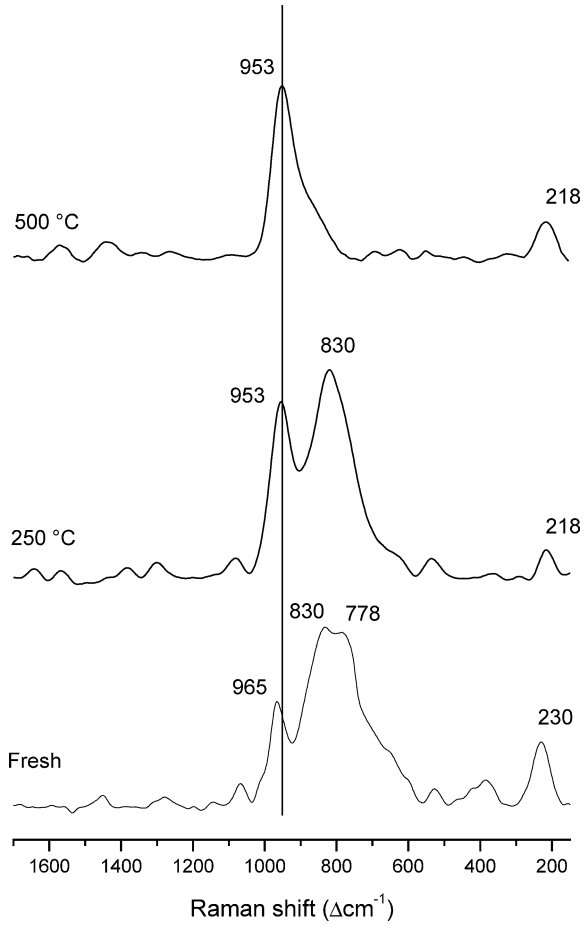

Fig. 5. Effect of thermal treatments of ZnMoP/γ-Al_2O_3 + TEG.

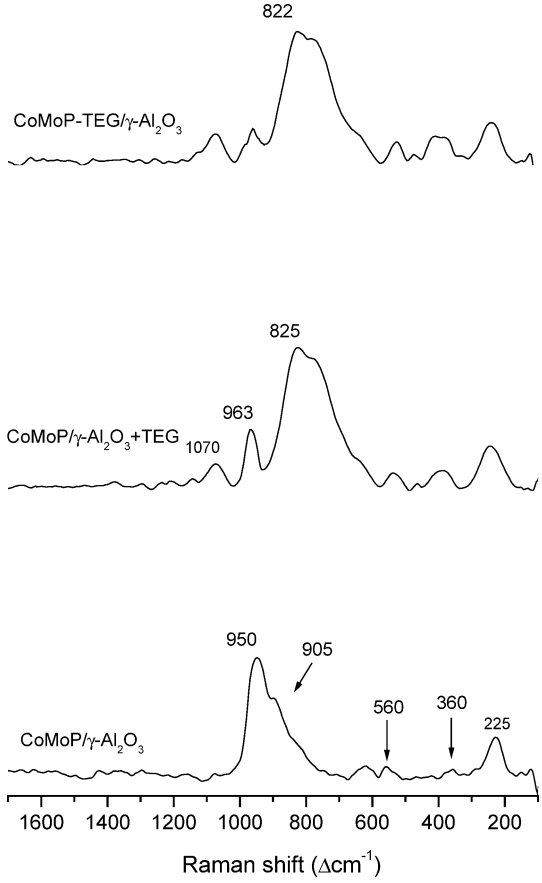

Fig. 6. Raman spectra of CoMoP-TEG/γ-Al_2O_3, CoMoP/γ-Al_2O_3 + TEG, and CoMoP-TEG/γ-Al_2O_3.

improve the quality of the spectra by measuring at liquid nitrogen temperature, we could not obtain better results.

To confirm that the main signal at 830 cm^{-1} arose from TEG, we calcined the ZnMoP/γ-Al_2O_3 + TEG sample at 250 and 500 °C for 3 h and collected the LRS spectra of the resulting samples. Fig. 5 shows the LRS spectra of the calcined samples together with the ZnMoP/γ-Al_2O_3 + TEG sample dried at 120 °C. After heating at 500 °C, the peak at 830 cm^{-1} disappeared, and the resulting spectrum showed the presence of heptamolybdate only.

The use of cobalt instead of zinc had no influence on the LRS spectra of the corresponding Co-containing samples (Fig. 6). $Al(OH)_6Mo_6O_{18}^{3-}$ was detected in the CoMoP/γ-Al_2O_3 sample (band at 950 and shoulder at 905 cm^{-1}).

4. Discussion

The presence of TEG in the phosphate-doped Zn(Co)Mo catalysts supported on alumina affects the structural properties of the oxidic metal precursors. The reaction between phosphate and molybdate in aqueous solution leads to the formation of the $P_2Mo_5O_{23}^{6-}$ heteropolymolybdate species. Cations in the solution together with the heteropolymolybdate species may be complexed as counter ions. We previously reported that the ^{31}P NMR spectrum of a solution containing diphosphopentamolybdate and Co(II) showed a strong paramagnetic effect, suggesting the formation of a Co-diphosphopentamolybdate species [11].

During impregnation of the γ-Al_2O_3 support, the phosphomolybdate species decompose to phosphate and heptamolybdate [7,8]. At low P loading (<2 wt%) the adsorption of phosphate usually leads to monophosphate, whereas molybdenum can be present as monomolybdate (Mo loading <12 wt%) or as heptamolybdate on the surface of the alumina support [20]. TEG interacts strongly with the alumina support and may inhibit the full decomposition of the phosphomolybdate species formed in the impregnation solution [11]. The ^{31}P NMR spectrum of a PO_4/γ-Al_2O_3 reference sample (with 1.5 wt% P), prepared by impregnating the dry support with a diluted solution of H_3PO_4, showed a broad signal centered at −8 ppm (Fig. 1). As reported herein, this signal arises from monophosphate. The same result was obtained for ZnMoP/γ-Al_2O_3 and CoMoP/γ-Al_2O_3 (Figs. 1 and 3). The ^{31}P NMR spectrum of the ZnMoP/γ-Al_2O_3 sample (Fig. 1) showed that phosphorus is present as monophosphate on the support. However, in the presence of TEG, the broad signal shifted to −9.6 ppm, and thus polyphosphate was detected. The adsorption of phosphate on γ-Al_2O_3 was studied extensively by van Eck et

al. [14]. Their ^{31}P and ^{27}Al NMR results showed that the polymerization of phosphate is favored when the support cannot accommodate phosphate as a monolayer. By comparing the BET surface area and the pore volume of bare γ-Al_2O_3 and the γ-Al_2O_3 + TEG sample (Table 1), it becomes clear that TEG causes a decrease in the surface area and pore volume and thus favors the formation of polyphosphate.

The ^{31}P NMR results on the Zn-containing samples proved that TEG not only favors the polymerization of phosphate, but also leads to the formation of the Keggin-type heteropolymolybdate species $PMo_{12}O_{40}^{3-}$. The Mo/P ratio of this species is 12. The deconvolution of the ^{31}P NMR spectra (Table 2) showed that the phosphorus atoms give rise to about the same amount of the heteropolymolybdate species in both the Zn- and TEG-containing samples. However, 15% of the phosphorus bound to Mo as $PMo_{12}O_{40}^{3-}$ is not sufficient to account for the total amount of molybdenum. From the initial ratio of Mo/P = 2.5, the percentage of Mo atoms that form $PMo_{12}O_{40}^{3-}$ species should be $(15 \times 12/2.5) = 72\%$. Therefore, the rest of the Mo might be present in the form of $Al(OH)_6Mo_6O_{18}^{3-}$.

During the impregnation step, $P_2Mo_5O_{23}^{6-}$ reacts with the alumina surface to form phosphate and MoO_4^{2-} [8]. Whereas phosphate reacts with acidic OH_s Al sites, MoO_4^{2-} preferentially reacts with basic sites [9]. We previously showed that TEG reacts with the basic OH_s Al sites, thus inhibiting the adsorption of $P_2Mo_5O_{23}^{6-}$ [11]. When impregnating γ-Al_2O_3 with the TEG-containing solution, $P_2Mo_5O_{23}^{6-}$ and TEG compete for the same adsorption on the alumina sites. When $P_2Mo_5O_{23}^{6-}$ adsorbs first, it decomposes and phosphate adsorbs on acidic OH_s Al sites [9]. The adsorption of molybdate is more complicated, because TEG adsorbs on the basic OH_s Al sites as well. When TEG blocks the basic OH_s Al sites, there are fewer sites available for the molybdate released by the decomposition of $P_2Mo_5O_{23}^{6-}$. This causes a decrease in the adsorption probability of molybdate; as a result, the local Mo/P ratio of the impregnation solution increases. This might explain the formation of the $PMo_{12}O_{40}^{3-}$ species. The fact that this species has also been detected in ZnMoP/γ-Al_2O_3 + TEG suggests that it is more stable on the surface film formed by TEG.

LRS spectra of the corresponding Co-containing samples (Fig. 6) suggested that the chemical state of molybdenum is the same for both systems. Thus, Zn-containing samples seem to be good model systems for the Co-containing samples. The LRS spectra provided in this work are not used for the speciation of molybdate in these very complex systems, but give us an idea of the similarity of the two systems. ^{27}Al NMR experiments carried out on our samples (results not given here) showed only the two typical Al bands corresponding to the tetrahedral and octahedral geometry of γ-Al_2O_3, as was expected given the fact that our systems are composed mostly of γ-Al_2O_3. The Anderson-type $AlMo_6$ structure is expected to be present in very small amounts on the alumina surface, thus giving rise in the ^{27}Al NMR to an extremely small signal compared to that from γ-Al_2O_3. Moreover, the presence of side bands in the spectra makes the search for such a small signal almost impossible. Therefore, in our opinion, classic ^{27}Al NMR experiments are not useful for investigating the presence of the Anderson-type $AlMo_6$ structure on the alumina surface. An alternative NMR technique that would exclude most of the bulk Al atoms from the spectra is the cross-polarization ^{27}Al MAS NMR, as used by Carrier et al. [19]. However, the purpose of the present study was to investigate the effect of TEG on both promoter atom and Mo in the phosphate-doped catalyst precursors.

The ^{31}P NMR spectrum of the CoMoP/γ-Al_2O_3 sample shows only one phosphorus signal centered at about −8 ppm, indicating the presence of monophosphate. The ^{31}P NMR spectra of the Co and TEG-containing samples show only one broad signal at around −9.5 ppm, indicating the formation of polyphosphate. No signal arising from the heteropolymolybdate was detected.

The presence of paramagnetic Co instead of diamagnetic Zn cations caused broadening of the heteropolymolybdate signals in the ^{31}P NMR spectra of the Zn-containing samples. This suggests that Co is in close proximity to the heteropolymolybdate species and proves that in the presence of TEG, a higher number of cobalt atoms are complexed by the phosphomolybdate species. This may lead to the formation of a more homogeneous Co–Mo–S type II structure and to a better performance of the final sulfided catalyst.

5. Conclusion

Using phosphate and TEG in the preparation of CoMo catalysts leads to an increase in the HDS activity. We previously showed that phosphate in the impregnation solution acts as a carrier of cobalt and molybdate by forming a protonated cobalt-diphosphopentamolybdate anion that decomposes into polyphosphate and molybdate during the impregnation of γ-Al_2O_3 [11]. PO_4 is present as monophosphate, whereas molybdate further reacts with alumina to form an Anderson-like aluminum molybdate species. NMR experiments are in progress to confirm this asset. By decreasing the surface area and pore volume of the γ-Al_2O_3, TEG favors the formation of polyphosphate. The structure of cobalt-diphosphopentamolybdate is not retained but is converted to a $PMo_{12}O_{40}^{3-}$ polymolybdate species. It is likely that this species is bound to the promoter atom. During sulfidation, this may lead to a better decoration of the promoter on the final MoS_2 slabs, thus explaining the improvement in the catalytic performance of these catalysts.

Acknowledgments

The authors thank Anuji Abraham for her kind help with the NMR measurements. This project was supported by the Swiss National Science Foundation.

References

[1] R. Iwamoto, J. Grimblot, Adv. Catal. 44 (2000) 417.
[2] R. Cattaneo, T. Weber, T. Shido, R. Prins, J. Catal. 191 (2000) 225.
[3] M. Sun, D. Nicosia, R. Prins, Catal. Today 86 (2003) 173.
[4] L. Pettersson, I. Andersson, L.O. Ohman, Acta Chem. Scand. A 39 (1985) 53.
[5] L. Pettersson, I. Andersson, L.O. Ohman, Inorg. Chem. 25 (1986) 4726.
[6] A. Griboval, P. Blanchard, E. Payen, M. Fournier, J.L. Dubois, Stud. Surf. Sci. Catal. 1061 (1997) 81.
[7] A. Griboval, P. Blanchard, E. Payen, M. Fournier, J.L. Dubois, Catal. Today 45 (1998) 277.
[8] W.C. Cheng, N.P. Luthra, J. Catal. 109 (1988) 163.
[9] J.A.R. van Veen, P.A.J.M. Hendriks, E.J.G.M. Romers, R.R. Andrea, J. Phys. Chem. 94 (1990) 5282.
[10] H. Kraus, R. Prins, J. Catal. 164 (1996) 251.
[11] E. Yamaguchi, Y. Uragami, H. Yokozuka, K. Uekusa, T. Yamaguchi, S. Abe, T. Kamo, T. Suzuki, European Patent Application 0601722 B1 (1998), to Sumitomo Metal.
[12] D. Nicosia, R. Prins, J. Catal. 229 (2005) 424.
[13] E.C. De Canio, J.C. Edwards, T.R. Scalzo, D.A. Storm, J.W. Bruno, J. Catal. 132 (1991) 498.
[14] H. Kraus, R. Prins, J. Catal. 170 (1997) 20.
[15] E.R.H. van Eck, A.P.M. Kentgens, H. Kraus, R. Prins, J. Phys. Chem. 99 (1995) 16080.
[16] T. Okura, N. Mizuno, M. Misono, Adv. Catal. 41 (1996) 113.
[17] A.K. Cheetham, N.J. Clayden, C.M. Dobson, R.J.B. Jakeman, J. Chem. Soc., Chem. Commun. (1986) 195.
[18] M.N. Harris, C.M. Bertolucci, L.J. Ming, Inorg. Chem. 41 (2002) 5582.
[19] L. Lyhamn, L. Pettersson, Chem. Scripta 12 (1977) 142.
[20] X. Carrier, J.F. Lambert, M. Che, J. Am. Chem. Soc. 119 (1997) 10137.